An investigation of the collective oscillations of a bubble cloud

S. W. Yoon[a] and L. A. Crum
National Center for Physical Acoustics, The University of Mississippi, University, Mississippi 38677

A. Prosperetti and N. Q. Lu
Department of Mechanical Engineering, The Johns Hopkins University, Baltimore, Maryland 21218

(Received 23 April 1990; accepted for publication 21 September 1990)

It is well known that ocean ambient noise levels in the frequency range from a few hundred hertz to several tens of kilohertz are well correlated with wind speed. A physical mechanism that could account for some of this sound generation is the production of bubble clouds by breaking waves. A simple laboratory study of the sound generated by a column of bubbles is reported here. From measurements of the various characteristics of this column, good evidence is obtained that the bubbles within the column are vibrating in a collective mode of oscillation. Based upon an assumption of collective oscillations, analytical calculations of the predicted frequency of vibration of this column as well as the dependence of this frequency on such parameters as bubble population and column geometry agree closely with the measured values. These results give evidence that the bubble plumes generated by breaking waves can be a strong source of relatively low frequency (<1 kHz) ambient noise.

PACS numbers: 43.30.Nb

INTRODUCTION

The literature contains substantial evidence that oceanic ambient noise is wind-dependent down at least to frequencies of a few hundred hertz.[1-3] The nature of the source of these low-frequency acoustic emissions is, however, still obscure. In view of this seeming correlation with breaking waves, it was suggested independently by Carey[4-6] and Prosperetti[7-9] that the collective oscillations of *bubble clouds* could explain these emissions. It is the purpose of the present paper to present an experimental confirmation of this possibility, and to show that analytical predictions agree closely with the measurements.

It is well known that bubbles abound in the first several meters under the ocean surface. Their origins are varied (impact of splashes, sprays, rain drops, biological activity, capillary waves of limiting form, and other mechanisms), but probably the most significant source of these bubbles is the breaking of surface waves.[10-12] The precise nature of the mechanism of air entrainment in a breaking wave is still poorly understood,[13] but it is plausible that at the moment at which the liquid surface closes on itself to entrap bubbles, its local velocity is nonzero. The bubble created in this way has therefore some initial kinetic energy and, unless it is spherical and with a balanced initial pressure, some initial potential energy as well. Since a bubble may roughly be regarded as a mechanical oscillator, one expects this initial energy to give rise to volume pulsations with associated acoustic emissions. The reason why such a simple picture is unacceptable as an explanation for the observed low-frequency noise is that the natural angular frequency ω_0 of a bubble of radius a is given approximately by

$$\omega_0 = (1/a)(3\gamma p_0/\rho)^{1/2},$$

where p_0 is the ambient pressure, ρ is the water density, and γ is the ratio of specific heats. With $p_0 = 10^5$ Pa, $\rho = 10^3$ kg/m^3, $\gamma = 1.4$, this relation would require a radius of about 7 mm for a frequency $f = \omega_0/2\pi = 500$ Hz, and it is by no means clear—and actually rather unlikely—that such large bubbles are created in significant numbers.

The collective oscillation hypothesis circumvents this problem by appealing to the well-known fact that a system of coupled oscillators (such as the bubbles in the cloud, for which the coupling is provided by mutual hydrodynamic and acoustic interaction) possesses normal modes the frequencies of which can be substantially lower than the natural frequencies of the individual oscillators. An intuitive argument leading to the same conclusion is as follows. It is well known that a mixture of air bubbles and liquid has a sound speed much lower than that of the pure liquid even at gas volume fractions as low as 1%. As a rough approximation, one can therefore consider a bubble cloud as an acoustic medium surrounded by a rigid enclosure, a system which is capable of normal modes of oscillation depending on its linear dimensions. Since the surrounding liquid is not, however, a rigid enclosure, the energy trapped in the cloud will "leak out" and be detectable as acoustic waves away from the bubble cloud. A very simple argument shows that the ratio of the minimum cloud eigenfrequency ω_m to the natural frequency ω_0 of the constituent bubbles (assumed to be equal) is of the order of[14]

$$\omega_m/\omega_0 \sim 1/\beta^{1/6} N_b^{1/3},$$

where β is the gas volume or void fraction in the cloud and N_b is the total number of bubbles. For example, a region with linear dimensions of the order of 10 cm and a void fraction of 1% could contain enough 1 mm radius bubbles to cause a frequency reduction of one order of magnitude.

The theoretical literature on bubble cloud collective-oscillation phenomena has seen several contributions in the last few years.[4-9,14-17] However, so far, no direct experimen-

[a] On leave from the Sung Kyun Kwan University, Seoul, Republic of Korea.

 0001-4966/91/020700-07$00.80

tal confirmation of the phenomenon has been reported. Here, we provide such a confirmation for clouds of cylindrical shape. Although this geometry is not of direct relevance to oceanic conditions, the verification of the concept and the very close agreement with theory are important steps toward the ultimate experimental proof.

I. EXPERIMENTAL PROCEDURE

We discovered that it was not easy to produce bubble "puffs" with a constant void fraction. It was too difficult to initiate or to terminate the bubble production quickly enough to generate reproducible geometric shapes. To avoid this problem, we chose to make bubble-filled columns which had a constant flux of air and thus also of bubbles. With these bubble columns, we were able to maintain a constant void fraction within a fixed geometrical configuration. Furthermore, the void fraction of the bubble column could be varied precisely by adjusting the flow rate through the flowmeter in the supply line to the bubble maker. A schematic diagram of the experimental apparatus is shown in Fig. 1.

A. Apparatus

To make the bubble column, a bubble maker was designed which consisted of forty-nine 22-gauge hypodermic needles with their tips cut off square. The needles were arranged in a circular cross-section to produce cylindrical clouds; an inset in Fig. 1 shows the geometry of the bubble maker. To ensure that each needle was provided with the same air pressure, the individual needles were connected by separate tubings with a manifold to an air-supply system. A stopcock for each tubing in the manifold was used to control air flow to the individual needles. To eliminate mechanical noise sources, compressed air was used as the air supply system for the bubble maker. The air flow through the pressure regulator and metering valve could be adjusted very precisely by using a high-resolution flowmeter (Cole-Parmer N-03227-22) that could measure flow rates from 0 to 80 ml/s with a precision of about 0.5 ml/s. The 49 hypodermic needles that comprised the bubble maker were arranged in concentric circles, with 1 needle at the center, 8 at the first radius, 16 at the second, and 24 at the third. The radii of the three circles were 2, 4, and 6 cm, respectively.

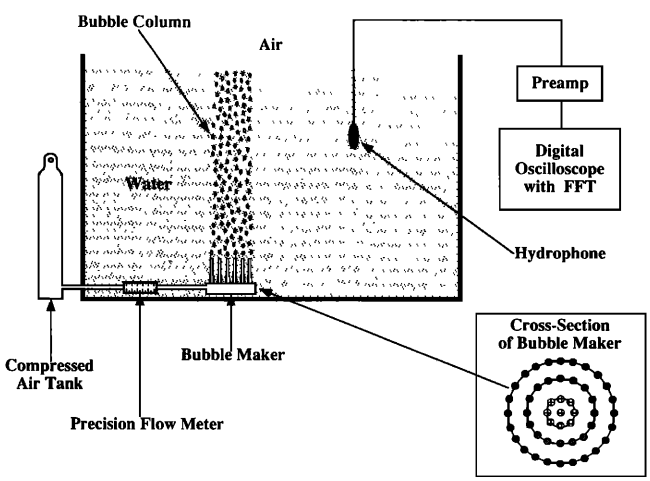

FIG. 1. Diagram of experimental apparatus. In order to generate bubble columns of different radii and void fraction, various combinations of needles in the bubble maker were activated.

B. Data acquisition

The column resonance frequency was measured with a hydrophone (B&K 8103) plus a charge amplifier (B&K 2635) connected to a dual-channel digital oscilloscope (LeCroy 9400). The hydrophone was installed midway down but outside the bubble column. These measurements were carried out either in a small water tank of dimensions $1\times1\times1$ m^3, or in a larger tank with dimensions $5\times5\times1.2$ m^3.

For noise spectrum analyses, the FFT algorithm and power spectrum averaging capability of the LeCroy 9400 digital storage oscilloscope were used. For averaging the spectra, 50 sweeps were used for each data point. For gathering preliminary data the Nyquist frequency was 6.24 kHz with a transform size of 2500 points. The frequency interval used was 20 Hz. For gathering final data, 1.25 kHz was set as the Nyquist frequency, also with a transform size of 2500 points. The frequency interval was 4 Hz. The standard deviations of the bubble column resonance frequencies were less than 2% for 50 spectrum averages. Shown in Fig. 2 are

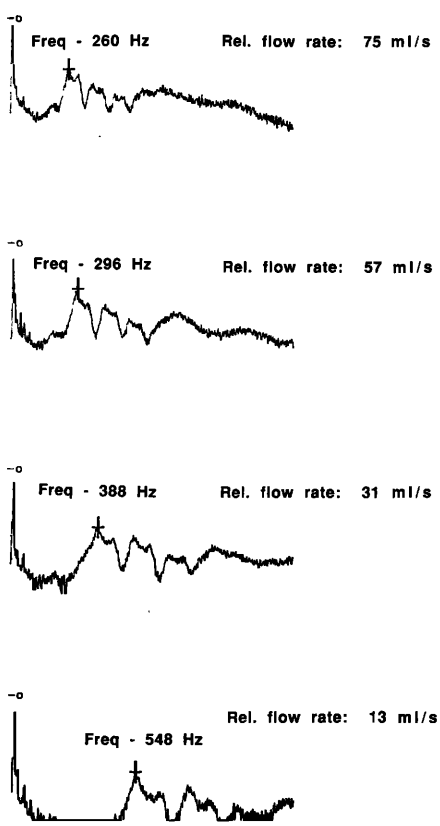

FIG. 2. Raw data showing the FFT spectra from the digital oscilloscope. The cursor indicates the location of the lowest bubble column resonance studied here. Also shown on the four different examples are the measured resonance frequencies for four different air flow rates. Note the shift to higher frequencies as the flow rate (proportional to void fraction) is reduced.

the averaged noise frequency spectra for a variety of air flow rates to the bubble maker. We have determined that the lowest peak (identified on the figure with the cursor) represents the lowest-mode frequency resonance of the bubble column. It is seen in this figure that as the air flow rate is reduced, the lowest resonance frequency of the column is elevated. We now present a brief theoretical analysis of the experimental condition described; later, a more detailed description of the various experiments that were performed to investigate these column resonances, as well as the major results of our study, will be given.

II. THEORY

The theoretical framework used to analyze the data has been presented in detail in Refs. 14, 18, and 19, and only a brief summary will be given here. The liquid-bubble mixture is described by means of averaged equations that lead, for the average pressure field P, to an effective Helmholtz equation of the form

$$\nabla^2 P + k_m^2 (P - p_0) = 0, \tag{1}$$

where p_0 is the undisturbed static pressure and, for equal-sized bubbles, the wave number k_m is given by

$$k_m^2 = \frac{\omega^2}{c^2} + \frac{4\pi\omega^2 an}{\omega_0^2 - \omega^2 + 2ib\omega}. \tag{2}$$

Here, ω is the angular frequency, c is the speed of sound in the pure liquid, a is the bubble radius, and $\omega_0(a)$ and $b(a)$ are the natural frequency and damping constant of a bubble of radius a, respectively.[18] The number density of the bubbles per unit volume n is related to the void fraction β by

$$\beta = \tfrac{4}{3}\pi a^3 n. \tag{3}$$

The acoustic disturbance in the pure liquid is described by an equation similar to (1), with k_m replaced by $k = \omega/c$. The boundary between the bubbly region and the pure liquid is treated as a geometrical surface on which the continuity of pressure

$$P = P^0, \tag{4}$$

and normal velocity

$$\mathbf{n}\cdot\nabla P = \mathbf{n}\cdot\nabla P^0, \tag{5}$$

are imposed. Here, P^0 denotes the pressure in the pure liquid.

To apply this theoretical framework to the experiment described in the previous section, we make a number of simplifying assumptions. We take the cloud to be cylindrical with an effective radius R_c and the tank to be a rigid concentric cylinder with a radius R_E. It will be shown that the theoretical results depend very weakly on this quantity and we therefore do not expect a significant error from this schematization. The vertical structure of the fields is taken to be proportional to

$$P - p_0 \propto \sin[N\pi(h - z)/2h], \tag{6}$$

where h is the depth of the needle's tips below the free surface and z is measured from these tips. This relation implies a pressure-release boundary condition at the surface of the tank. If N is an odd integer, in particular $N = 1$, the plane $z = 0$ is treated like a rigid boundary, while if N is an even integer, in particular $N = 2$, it effectively behaves as a pressure-release boundary. Noninteger values of N may be used to simulate intermediate cases. As will be described in Sec. III, the data indicate that the value $N = 2$ describes the situation rather closely.

The calculation of the normal modes for this system proceeds in a very straightforward way. Since the pressure field in the mixture must be finite on the axis $r = 0$ of the bubble column, it follows from (6) that it must have the form

$$P - p_0 = e^{im\theta} J_m\left[r\sqrt{k_m^2 - (n\pi/2h)^2}\right] \times \sin[N\pi(h - z)/2h], \tag{7}$$

where, in view of the linearity of the problem, a unit amplitude has been assumed and J_m is the Bessel function of order m. The index m describes the azimuthal structure of the field. The case $m = 0$ corresponds to axially symmetric conditions, a situation that seems to prevail in the experiment. The corresponding solution in the pure liquid has the form

$$P^0 - p_0 = e^{im\theta} \sin[N\pi(h - z)/2h] \times \{A_m H_m^{(1)}\left[r\sqrt{k^2 - (N\pi/2h)^2}\right] + B_m H_m^{(2)}\left[r\sqrt{k^2 - (N\pi/2h)^2}\right]\}, \tag{8}$$

where $H_m^{(1)}$ and $H_m^{(2)}$ are the Hankel functions of first and second kinds of order m, respectively. A relation between the amplitudes A_m and B_m can be obtained by imposing vanishing velocity at the tank wall $r = R_E$. One of the conditions (4) or (5) at $r = R_c$ determines then the remaining amplitude while the other condition, i.e., (5) or (4), gives the characteristic equation in the form

$$x\,[J_{m-1}(x)/J_m(x)] = s\,\frac{H_{m-1}^{(2)}(s)/H_m^{(2)}(s) - \tilde{H}_m\,[H_{m-1}^{(1)}(s)/H_m^{(1)}(s)]}{1 - \tilde{H}_m}, \tag{9}$$

where

$$x = R_c\sqrt{k_m^2 - (N\pi/2h)^2}, \quad s = R_c\sqrt{k^2 - (N\pi/2h)^2}, \tag{10}$$

and

$$\tilde{H}_m = \left[\frac{H_{m-1}^{(2)}(y)/H_m^{(2)}(y) - m/y}{H_{m-1}^{(1)}(y)/H_m^{(1)}(y) - m/y}\right] \times \left[\left(\frac{H_m^{(1)}(s)}{H_m^{(2)}(s)}\right)\left(\frac{H_m^{(2)}(y)}{H_m^{(1)}(y)}\right)\right], \tag{11}$$

with

$$y = R_E\sqrt{k^2 - (N\pi/2h)^2}. \tag{12}$$

For the axisymmetric mode m = 0 these relations become

$$xJ_1(x)/J_0(x) = s\,\frac{H_1^{(2)}(s)/H_0^{(2)}(s) - \tilde{H}_0\,[H_1^{(1)}(s)/H_0^{(1)}(s)]}{1 - \tilde{H}_0}, \tag{13}$$

where

$$\tilde{H}_0 = [H_1^{(2)}(y)/H_1^{(1)}(y)]\,[H_0^{(1)}(s)/H_0^{(2)}(s)]. \tag{14}$$

The numerical solution of the eigenvalue equation (9) or (13) is rather involved and is described in Refs. 14 and 19.

It may be noted that the results are rather insensitive to the precise nature of the boundary conditions at $r = R_E$. A change from a rigid to a "soft" (i.e., $P = p_0$) boundary has hardly any effect on the results shown below.

III. RESULTS AND DISCUSSION

A. Void fraction

The void fraction, i.e., the ratio of air volume to the total volume of the bubble column, can be determined from the amount of air flowing into the column. If the number of needles open in the bubble maker remains constant, then the void fraction of the bubbly mixture can be computed from the following relation:

$$\beta = \dot{V}t/Sh, \tag{15}$$

where $\dot{V}$ is the total air volume flow rate, t is the time for a bubble to rise from the bubble maker to the water surface, S is the effective cross-sectional area of the bubble column, and h is its height. The effective cross-sectional area of the bubble column can be determined by observation, either directly with the eye or through simple photography. The bubble rise time was measured by cutting off the air supply for a short time during an otherwise steady state and then rapidly starting the air flow and measuring the time required for the front of the bubbly mixture to reach the tank water surface. Because of liquid entrainment into the column by the rising bubbles, the rise time depended on the void fraction; thus, for each air flow rate, a separate rise time measurement was performed in order to determine the correct value of the void fraction. The column height and cross section were measured and found to be nearly independent of air flow rate.

To confirm our measurements of the void fraction, a photo technique was used as an independent determination of this quantity. By making photographs of the bubble columns at given air flow rates, the actual bubble population was determined for the bubbly mixture. This laborious method was used only to confirm the estimates based on (15) and was not used to determine the data points in the figures to follow, unless specifically mentioned.

We show in Fig. 3 a photograph of a typical bubble column. Note that the bubbles are nearly the same size but more oblate than spherical, there is little if any coalescence, the bubbles are evenly distributed, and the edges of the column are reasonably well defined. With our bubble maker we could maintain a constant and stable flux of bubbles. The bubble radius was somewhat dependent on the air flow rate and increased approximately from 1.5 to 2.4 mm as the air flow rate was increased.

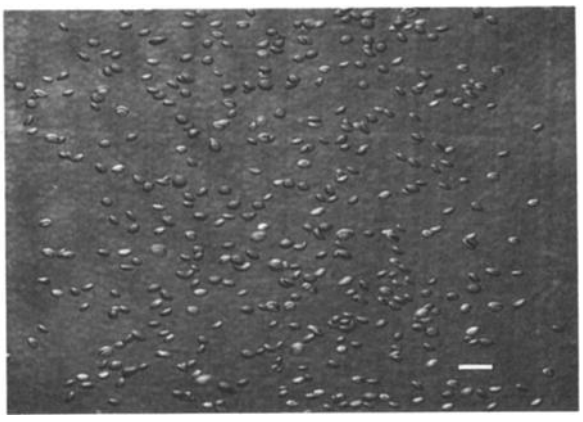

FIG. 3. Photograph of a typical bubble column. For this case 45 needles were open, the flow rate per needle was about 30 ml/min and the average bubble size was about 1.6 mm. The length of the bar for a scale is 1 cm.

B. Bubble column resonance

We investigated the dependence of the bubble column resonance frequency on the void fraction for various column radii. The physical cross-sectional area of the bubble maker could be set at radii of 6.0, 4.0, or 2.0 cm. However, the effective cross-sectional area was larger than the physical cross-sectional area because of zigzag rising motions of individual bubbles, and effective bubble column radii of 7.0, 5.4, and 4.6 cm were measured from photographs in the three cases.

To demonstrate that a standing wave does exist within the bubble column, we probed its interior with a small hydrophone. These results are shown in Fig. 4 which displays the amplitude of the acoustic pressure as a function of hydrophone depth measured from the water surface. The tips of the needles are at a depth of 0.82 m. The smooth curve shown in this figure represents a sine wave with a half-wavelength of 0.85 m fitted to the data. This value is somewhat greater than the depth of submergence of the needle tips. On the other hand, the bottom boundary of the bubble column is not clearly defined. The bubble maker rests on the bottom of the tank which is made of 1.8-cm-thick plywood raised from the floor by means of wooden beams. The base of the needles is 5.5 cm above the bottom, and the total distance between the needles tip and the tank bottom is 10.5 cm. Given this experimental configuration, a pressure-release condition at the bottom of the column as suggested by the data of Fig. 4 is not unreasonable.

Shown in Fig. 5 is the dependence of the bubble column lowest resonance frequency (identified with the lowest peak

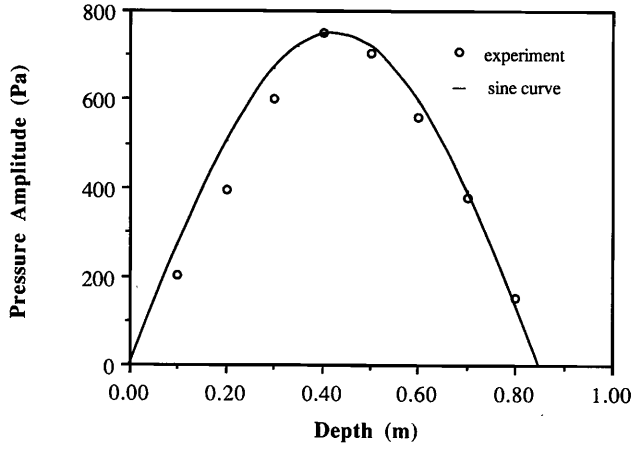

FIG. 4. Variation of the acoustic pressure amplitude within the bubble-filled column as a function of depth below the water surface for a fixed void fraction. The measured data are fitted with a sine curve, indicating a pressure-release boundary condition on both ends of the column.

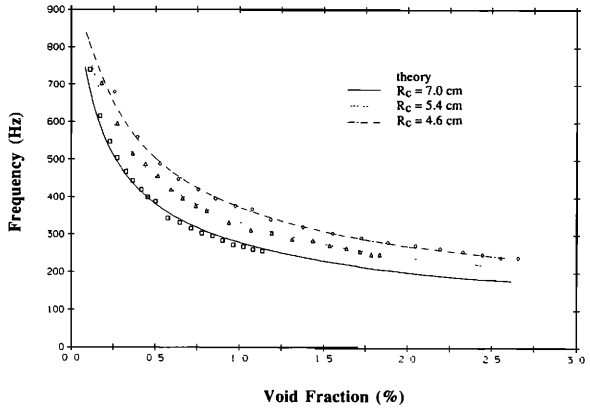

FIG. 5. Variation of the measured (various symbols) and theoretical (various curves) values of the bubble column resonance frequency with void fraction for three different column radii. The theoretical curves are obtained from Eq. (13). The column height was 0.82 m, the average bubble radius was 2.0 mm, and the distance to the tank walls from the center of the bubble column assumed in the theory was 0.75 m.

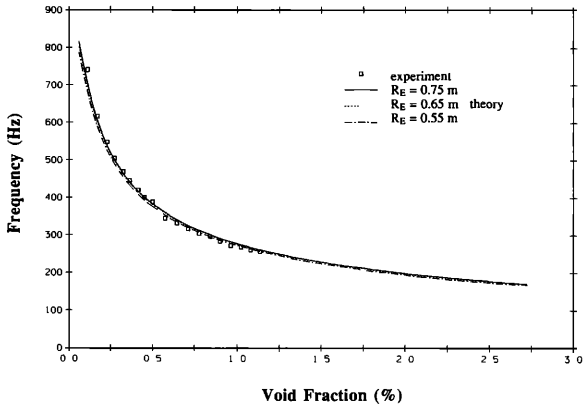

FIG. 6. Effect of the tank radius used in the calculation on the column resonance frequency. The theoretical curves are obtained from Eq. (13) in the text. The close proximity of the three curves indicates a weak dependence on the tank size. The theoretical calculations and experimental data are for an effective column radius of 7.0 cm, and a column height of 0.82 m; the tank size in this experiment was $5\times5\times1.2$ m^3 (LWH). (Compare Fig. 7.)

of the measured spectra shown in Fig. 2) on the void fraction for various column radii R_c. For case A, all 49 hypodermic needles were open (see Fig. 1), and the effective column radius was 7.0 cm; for case B, the outer ring was closed, the two interior rings were open, and the effective radius was 5.4 cm; for case C, both outer rings were closed, the remaining nine needles were open, and this arrangement lead to an effective radius of 4.6 cm. For all cases the air flow rates varied from about 1 ml/s to near 80 ml/s and the height of the bubble column was held constant at 0.82 m above the needle tips. The measurements for this figure were performed in tap water in a tank that measured $1\times1\times1$ m^3. It appears from these data that the broad-band noise of the bubbles exiting from the nozzles—in Longuet-Higgins' picturesque language: "their birthing wail"—is activating a standing wave in the column. As the void fraction is changed by increasing air flow, the speed of sound in the bubbly medium is diminished, resulting in a reduction in the frequency of the lowest mode.

Also shown in Fig. 5 are the results of the theoretical predictions based upon a numerical solution of the eigenvalue equation (13) above for the frequency of the lowest mode as a function of void fraction for the three (effective) column radii examined in the experiment. One sees an impressive agreement between predicted and measured values.

An obvious concern in analyzing these data was the effect of the tank lateral boundaries. In the theoretical analysis, we assume cylindrical symmetry and that lateral boundaries exist at a specified distance from the bubble column. In order to test experimentally the effect of the boundaries, we performed measurements in two separate tanks. Figures 6 and 7 show tests of the theoretical and experimental sensitivity to the boundaries of the tanks. First, in Fig. 6, a comparison is made between theory and experiment for a case in which the column height was 0.82 m and the effective cross sectional radius of the bubble column was 7.0 cm. These measurements were performed in our larger tank ($5\times5\times1.2$ m^3). The bubble column was not positioned in the middle of the tank but about 1.2 m away from one edge, and at about equal distances from the other two walls. The theoretical lines are for three cases in which the outer cylindrical surface used in the theoretical model has radii R_E of 0.75, 0.65, and 0.55 m. Note from these calculations that very little effect of the boundary is predicted.

These theoretical results are confirmed in an experimental test whose results are shown in Fig. 7. For this case, the variation in column frequency with void fraction was examined for a bubble column of 0.82-m height and 7.0-cm effective cross section, but in two separate tanks. The measurements in case AA were made in the large tank ($5\times5\times1.2$ m^3); those for case A were made in the small tank ($1\times1\times1$ m^3). In agreement with the theoretical predictions shown in the previous figure, very little tank dependence was observed.

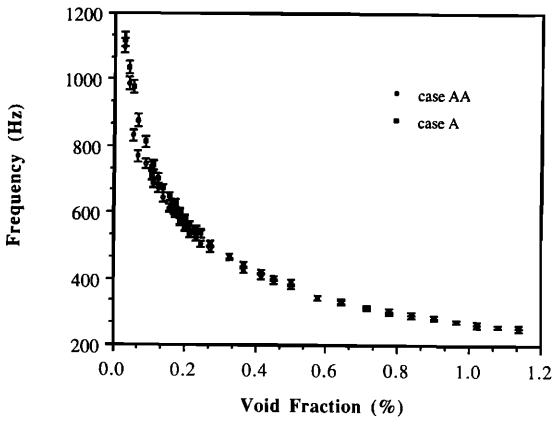

FIG. 7. Variation of the column resonance frequency with void fraction for two different tank sizes. In case AA, the size of the tank was $5\times5\times1.2$ m^3; in case A, the size of the tank was $1\times1\times1$ m^3 (LWH). These data and the corresponding calculation in Fig. 6 indicate a weak dependence on tank size.

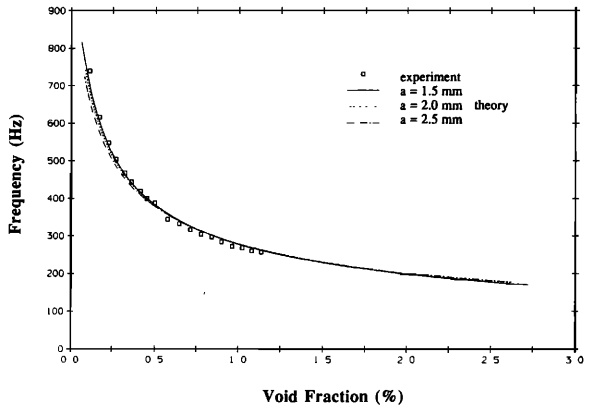

FIG. 8. Variation of the column resonance frequency with void fraction for three different values of the average bubble radius; the theoretical calculations are obtained from Eq. (13) in the text. The close proximity of the three curves indicate a weak dependence on the average size of the bubbles within the column. The theoretical calculations and the experimental data are for an effective column radius of 7.0 cm and a height of 0.82 m. The experimental data are for an average bubble radius of about 2.0 mm. (Compare Fig. 9.)

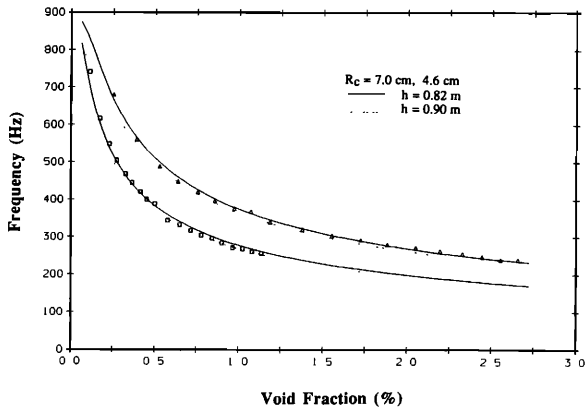

FIG. 10. Effect of the column height used in the calculation on the predicted lowest mode. The solid lines are for $h = 0.82$ m, as in all of the previous figures, while the dashed lines are for $h = 0.90$ m. The data are the same as shown in Fig. 5.

A final series of measurements were made to examine the effect of bubble size. Since the resonance frequency of the column is significantly different from the natural resonance frequencies of the individual bubbles, the important parameter in the resonance of our column is the void fraction, not the bubble size. We can demonstrate this prediction again with a combination of two figures, one principally theoretical in nature, the second principally experimental.

Shown in Fig. 8 are the theoretical results for bubble radii of 1.5, 2.0, or 2.5 mm. The data are the same ones shown in Figs. 5 and 6 for a column height of 0.82 m and an effective radius of 7.0 cm. The expected result is supported by the very small effect of the bubble radius on the theoretical curves.

To demonstrate the same effect experimentally, we exploited the dependence of the bubble radii on the air flow rate. By using flowrates of 30 ml/min and 60 ml/min per needle, we could generate bubbles with radii of 1.6 and 2.0 mm, respectively. In this case, in order to vary the void fraction, we varied the number of active needles of the bubble maker still trying to retain the geometry of the system as much as possible. For this set of experiments, in order to have more reliable measurements of the void fractions, it was necessary to take photographs of the column and count the bubbles. In Fig. 9, we show the results obtained in this way for a column height of 0.82 m and an effective cross-sectional radius of 7.0 cm. The data do not show any observable dependence on the bubble radius.

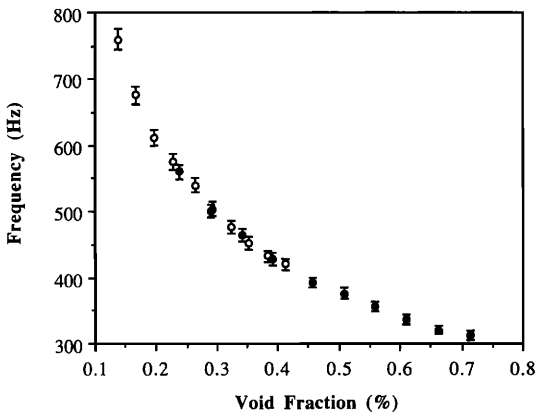

FIG. 9. Variation of the column resonance frequency with void fraction for two different flow rates that resulted in two different average bubble radii. For the flow rate of 30 ml/min to the individual needles (open circles), the average bubble size was about 1.6 mm; for the flow rate of 60 ml/min (closed circles), the average bubble size was 2.0 mm. In accordance with the theoretical predictions indicated in Fig. 8, there is a weak dependence on bubble size.

As a further test of the applicability of the theory to the present case we consider the sensitivity of the theoretical predictions to the height of the column which, as has been mentioned above, is not unambiguously defined in the present experimental situation. Figure 10 compares data and theory for the largest and smallest column radii. The two pairs of theoretical lines have been obtained assuming a column height of 0.82 m, as in the preceding figures, and 0.90 m, which is close to the total depth of the tank. It can be seen that the effect of this 10% change in column height is small and, therefore, that the imprecision with which h is known does not affect in any significant way the agreement between theory and experiment reported in this paper.

IV. CONCLUSIONS

By performing a relatively simple experiment, we have been able to demonstrate the existence of collective oscillations of bubble clouds. We have found that a bubble cloud can radiate sound at frequencies substantially lower than the natural frequency of the individual constituent bubbles. This result is consistent with a theoretical description of the cloud based on averaged equations in which the bubbly medium appears as a continuum endowed with effective bulk properties distinct from those of the individual bubbles or the pure liquid. We have also shown that this theory is in excellent agreement with the data. This circumstance gives confidence that the predictions of the theory would also be accu-

rate for situations not as easily amenable to experiment as the one studied here. In particular, this finding strengthens the suggestion[4-9] that most of the natural oceanic ambient noise below 1 kHz may be due to the oscillations of bubble clouds and plumes produced by breaking waves.

ACKNOWLEDGMENTS

This work was supported by the Office of Naval Research. The authors are grateful to K. J. Park for gathering some experimental data. One of the authors (SWY) received an oversea research grant from The Korea Science and Engineering Foundation.

[1] G. Wenz, "Acoustic ambient noise in the ocean: spectra and sources," J. Acoust. Soc. Am. **34**, 1936–1956 (1962).
[2] A. J. Perrone, "Deep ocean ambient noise spectra in the Northwest Atlantic," J. Acoust. Soc. Am. **46**, 762–770 (1969).
[3] B. R. Kerman, "Underwater sound generation by breaking waves," J. Acoust. Soc. Am. **75**, 149–165 (1984).
[4] W. M. Carey, "Low-frequency ocean surface noise sources," J. Acoust. Soc. Am. Suppl. 1 **78**, S1–S2 (1985).
[5] W. M. Carey, "Low frequency noise and bubble plume oscillations," J. Acoust. Soc. Am. Suppl. 1 **82**, S62 (1987).
[6] W. M. Carey and D. Browning, "Low-frequency ocean ambient noise: Measurements and theory," in *Sea Surface Sound*, edited by B. R. Kerman (Kluwer Academic, Norwell, MA, 1988).
[7] A. Prosperetti, "Bubble-related ambient noise in the ocean," J. Acoust. Soc. Am. Suppl. 1 **78**, S2 (1985).
[8] A. Prosperetti, "Bubble dynamics in oceanic ambient noise," in *Sea Surface Sound*, edited by B. R. Kerman (Kluwer Academic, Norwell, MA, 1988).
[9] A. Prosperetti, "Bubble-related ambient noise in the ocean," J. Acoust. Soc. Am. **84**, 1042–1054 (1988).
[10] S. A. Thorpe, "On the clouds of bubbles formed by breaking wind-waves in deep water, and their role in air–sea gas transfer," Phil. Trans. R. Soc. London Ser. A **304**, 155–210 (1982).
[11] E. C. Monahan, "Fresh water whitecaps," J. Atmos. Sci. **26**, 1026–1029 (1969).
[12] R. Hollet and R. W. Heitmeyer, "Noise generation by bubbles formed in breaking waves," in *Sea Surface Sound*, edited by B. R. Kerman (Kluwer Academic, Norwell, MA, 1988).
[13] M. S. Longuet-Higgins and J. S. Turner, "An entraining plume model of a spilling breaker," J. Fluid Mech. **63**, 1–20 (1974).
[14] N. Q. Lu, A. Prosperetti, and S. W. Yoon, "Underwater noise emissions from bubble clouds," IEEE J. Ocean Eng. **15**, 275–281 (1990).
[15] R. Omta, "Oscillations of a cloud of bubbles of small and not so small amplitude," J. Acoust. Soc. Am. **82**, 1018–1033 (1987).
[16] L. d'Agostino and C. Brennen, "Acoustical absorption and scattering cross sections of spherical bubble clouds," J. Acoust. Soc. Am. **84**, 2126–2134 (1988).
[17] S. W. Yoon, K. J. Park, L. A. Crum, M. Nicholas, R. A. Roy, A. Prosperetti, and N. Q. Lu, "Collective oscillations in a bubble column," in *Natural Physical Sources of Underwater Sound*, edited by B. R. Kerman (Kluwer Academic, Dordrecht, The Netherlands, 1990) (in press).
[18] K. W. Commander and A. Prosperetti, "Linear pressure waves in bubbly liquids: Comparison between theory and experiments," J. Acoust. Soc. Am. **85**, 732–746 (1989).
[19] N. Q. Lu and A. Prosperetti, "Acoustics of bubble layers," J. Acoust. Soc. Am. (to be published).